Available online at www.sciencedirect.com
SCIENCE DIRECT®
Journal of Photochemistry and Photobiology A: Chemistry 157 (2003) 127–136
Journal of Photochemistry and Photobiology A:Chemistry
www.elsevier.com/locate/jphotochem

Time-windowing Fourier transform absorption spectroscopy for flash photolysis investigations

Oliver C. Fleischmann [a,*], John P. Burrows [a], Johannes Orphal [b]

[a] *Institute of Remote Sensing, University of Bremen, 28356 Bremen, Germany*
[b] *Laboratoire de Photophysique Moléculaire, Université de Paris-Sud, F-91405 Orsay Cedex, France*

Received 30 May 2002; received in revised form 14 December 2002; accepted 17 January 2003

Abstract

A technique for recording time-resolved absorption spectra using a commercial continuous-scan Fourier transform spectrometer (FTS) is presented. The method has been designed for the observation of experiments at temporal resolutions from 10^{-4} to 10^{-2} s, with delays longer than a second between two experimental repetitions. This is accomplished by synchronizing the observed experiment to certain positions of the interferometer scanning mirror. Unlike other interleaving or stroboscopic techniques, a trigger is not generated for every interferogram point. Instead, time windows are used that are several interferogram points wide. For experiments with a low repetition rate (0.1–1 Hz), the approach has advantages concerning measurement time and spectral resolution when compared to the step-scan and to fast synchronized continuous-scan methods. The time-windowing Fourier transform spectrometer (TW-FTS) has been implemented as a hardware and software add-on to a commercial continuous-scan Michelson interferometer. No changes were made to the instrument. Two validation experiments were carried out by observing the formation and self-reaction of BrO after the flash photolysis of a Br_2/O_3 mixture at 298 K. The experimental concentration–time profiles were in good agreement with decay curves from a chemical kinetics simulation of the experiments. Further, a UV absorption spectrum of BrO, recorded by the TW-FTS method, had a comparable quality as a static FTS recording.

Keywords: Time-resolved spectroscopy; Fourier transform spectroscopy; Continuous-scan

1. Introduction

The Fourier transform spectrometer (FTS) is being used in various fields of optical measurements and spectroscopy. In the form of a Michelson interferometer, the FTS is found in many applications [1,2]. Compared to the widely used grating spectrograph, the FTS has several implicit advantages. These include the spectral resolution, the frequency calibration (Connes-advantage), the broad spectral range, and the optical throughput (Jacquinot-advantage) [3]. One general requirement for the FTS is the stability of experimental conditions during the recording of the interferogram. During one scan of the moving mirror in the Michelson interferometer, the light intensity needs to be constant. Therefore, we refer to the classic continuous-scan interferometer as the static FTS. The condition of constant light intensity makes the static FTS in many cases impractical for time-resolved observations. Here, the best temporal resolution that can be achieved is given by the duration of one scan.

Several techniques have been reported to enable time-resolved measurements with a Fourier transform spectrometer. Most of these methods have been used for emission studies and in the infrared spectral range. The rapid-scan FTS is a method for time-resolved FTS measurements, that is very similar to the classic continuous-scan. In the rapid-scan, the scan duration is minimized by the use of fast mechanical devices for the mirror movement. High-speed scanners can operate with a maximum repetition rate of 100 Hz at a spectral resolution of 16 cm^{-1} [4]. So, the best temporal resolution of a rapid-scan FTS is around 10 ms.

A completely different technique is the step-scan, introduced by Murphy and Sakai in 1978 [5] and Barowy and Sakai [6] and since then used in many studies [7–11]. For the step-scan, the mirror is stopped at a single sampling point of the interferogram. Then, the dynamic experiment is started, and the transient interference signal is recorded for the current optical path difference. This procedure has to be repeated for every sampling point. Finally, by resorting the data, a series of interferograms is yielded, each of which represent a particular time window. Note, that for the step-scan the number of repetitions of the experiment equals

* Corresponding author.
E-mail address: oliver-cf@gmx.de (O.C. Fleischmann).

1010-6030/03/$ – see front matter © 2003 Elsevier Science B.V. All rights reserved.
doi:10.1016/S1010-6030(03)00069-8

the number of sampling points in the interferogram. This can lead to very long measuring times when a high spectral resolution is required while the experimental repetition rates are very low. On the other hand, if repetition rates are very high, then a high spectral resolution together with a high temporal resolution can be achieved. This has recently been demonstrated by Picqué and Guelachvili [12] with a spectral resolution of 0.01 cm^{-1} and a temporal resolution of 500 ps.

Since the effort regarding the step-scan mechanics is quite high, several techniques have been reported to implement a time-resolved observation mode on a classic continuous-scan FTS [13–18]. These methods, known as synchronized continuous-scan techniques, achieve a temporal resolution that is below the duration of one scan. Both the step-scan and the synchronized continuous-scan make use of the fact that the interferogram is sampled digitally at discrete points of the optical path difference. In the synchronized continuous-scan, the dynamic experiment is started during the scan of the moving mirror. A trigger signal is produced, when the mirror reaches a certain optical path difference. This implies that the experiment has to be synchronized to the mirror movement. However, the existing variants of the synchronized continuous-scan have in common that, similar to the step-scan, the experiment has to be carried out once for every sampling point of the interferogram. As said before, this may cause long measuring times when the experimental repetition rate is low.

The problem can be overcome by sorting the interferogram samples of the continuous-scan into time windows. When the experimental conditions are not changing rapidly, several samples can be regarded as being in the same time window. Now, only one trigger for every 10–100 interferogram points is needed, and not for every single point. Since fewer repetitions are necessary, this approach allows the recording of medium to high resolution spectra within a reasonable measurement time even at low repetition rates.

Here we present the time-windowing Fourier transform spectrometer (TW-FTS). The technique was implemented on a commercial continuous-scan interferometer (Bruker IFS 120 HR). No hardware or software changes were necessary to the instrument, and the presented technique is expected to be easily adapted to various continuous-scan spectrometers. The new TW-FTS technique was developed for the dynamic observation of the atmospheric radical BrO in flash photolysis experiments. These experiments are characterized by a low repetition rate of about 0.1–0.15 Hz due to refilling of the sample chamber. Therefore, older techniques like the step-scan FTS or the existing methods of the synchronized continuous-scan FTS could not be employed. Moreover, due to time constants of typically between 1 and 10 ms, a rapid-scan FTS could not be used either.

The two main issues are kinetic studies of gaseous reactions involving BrO and the recording of reference ultraviolet absorption spectra of BrO for atmospheric remote sensing. Generally, these reference spectra should have a spectral resolution of better than 5 cm^{-1} [19]. So far, most studies of the UV absorption cross-section of BrO have employed grating spectrographs [20–23], where the best spectral resolution that can be achieved is around 0.20 nm (18 cm^{-1} at 30,000 cm^{-1}). Only two studies have used a Fourier transform spectrometer [24,25], and both of them used the FTS in static mode. In order to verify the usability of the presented TW-FTS technique for flash photolysis experiments, two validation experiments have been carried out. The well investigated Br_2 photosensitized decomposition of O_3 has been observed at room temperature. A more thorough study of the UV absorption cross-sections of BrO at stratospheric temperatures has been carried out after the validation of the TW-FTS method. While the TW-FTS technique is presented here in detail, the results for the UV absorption cross-sections of BrO are being published separately [26].

2. Measurement principle of TW-FTS

The TW-FTS concept is similar to the interleaved continuous-scan as described in [13]. It is based on the fact that there is a temporal order of the interferogram sampling points that are recorded in one scan. The temporal relations between the data points result from the movement of the scanning mirror. For a continuous-scan FTS, the period between two successive interferogram data points is typically between 10 and 100 μs. If the observed experiment exhibits dynamic processes during the recording of the interferogram, these processes will find their representation at certain positions in the interferogram. When a trigger pulse is generated at the time the scanning mirror passes a certain point of the interferogram, every sampling point has a definite temporal relation to this trigger point. If the trigger pulse is used to initiate a time-resolved experiment, particular points of the interferogram may be clearly associated with certain times during this experiment. The interleaved synchronized continuous-scan can be used, when the experimental time constants are between 10 μs and 100 ms. In this case, the transients can extend over many data points of the interferogram.

In order to obtain the complete information about the dynamic experiment, several interferograms have to be recorded. In each interferogram, the trigger must have a different position. In a complete set of interferograms, the trigger has to be moved all over the optical path difference. In earlier implementations of the synchronized continuous-scan, the trigger position was moved by one point in the interferogram [13,16,17]. Thus, as mentioned above, for every sampling point the experiment had to be executed once. However, for flash photolysis experiments, the experimental time constants are between 1 and 10 ms and hence much bigger than the temporal distance between two successive samples in the interferogram. In this case, several data points may be regarded to be in the same time window. The experimental conditions inside of one time window are assumed to be constant. The width of the time

windows defines the temporal resolution of the measurement. If, for example, the time windows are 100 points wide, the experiment has to be carried out only once for every 100 interferogram data points, and not for every single data point. Due to fewer experimental repetitions, the total measuring time is reduced significantly. Because of the establishing of time windows, we called the new method TW-FTS.

From the complete set of interferograms, the spectral information for every time window can be extracted. For each time window, the corresponding sections are cut out of every recorded interferogram. All slices, put together in one single vector, form the new time window interferogram. Here it is assumed that only one trigger is generated per interferometer scan. This is also the case for our flash photolysis experiments where the long relaxation time of typically 7.5 s is longer than the scan duration of around 1–5 s. For experiments exhibiting a faster repetition rate, it is possible to set up several triggers during one scan. By doing this, the total measurement time can be decreased considerably.

Figs. 1 and 2 illustrate the relations of raw data and time window interferograms in an example with 201 interferograms. Fig. 1 shows three representative raw interferograms, as they have been recorded by the FTS. The numbering of

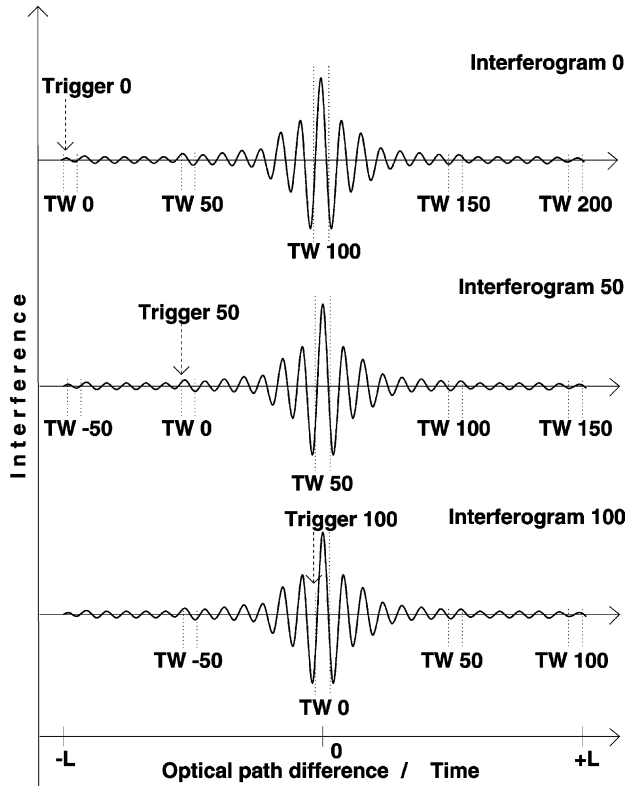

Fig. 1. Interferogram raw data from a typical TW-FTS measurement with a total of 201 dynamic interferograms. Three representative scans are drawn. The position of the generated trigger during the scan is marked as well as some of the time windows (TW). The experimental times are measured relative to the trigger.

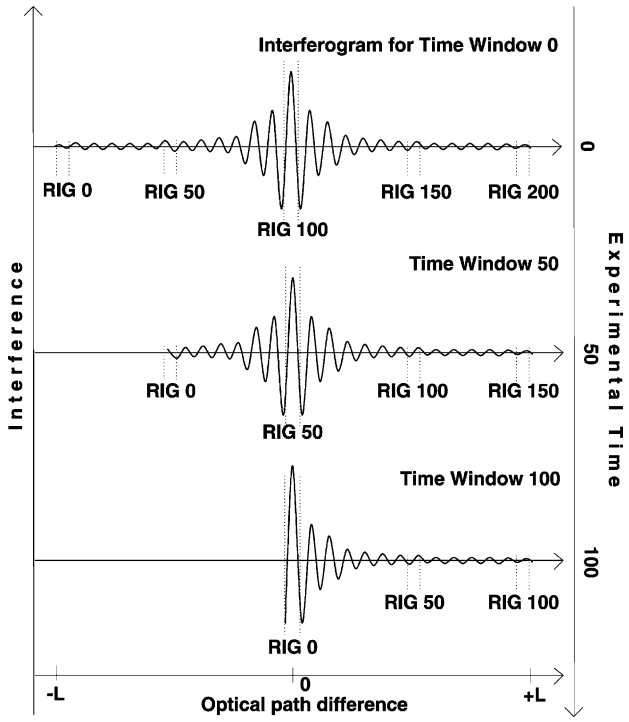

Fig. 2. Time window interferograms of the TW-FTS example resulting from processing of the raw data (Fig. 1). The temporal axis is vertical now, in difference to Fig. 1. The abbreviation RIG indicates, in which of the raw interferograms the data samples have been recorded.

interferograms and time windows starts at 0. The horizontal axis in Fig. 1 represents the optical path difference as well as the experimental time. These two variables are connected through the velocity of the scanning mirror. The optical path difference is assumed to vary linearly with the experimental time. In a real experiment, the relation is not exactly linear, and it has to be characterized by a calibration measurement. The vertical axis corresponds to the magnitude of the interference. The trigger points are moved to the right (forward) for every subsequent scan. The locations for the time windows 0, 50, 100, 150, and 200 are marked schematically in the raw interferograms of Fig. 1. The moment when the trigger is generated is defined as time 0.

Before calculating the spectra, time window interferograms have to be generated from the raw interferograms. In Fig. 2, some representative time window interferograms are drawn, corresponding to the raw data from Fig. 1. From these new interferograms, the proper spectra for each time window may be calculated. The horizontal axis in Fig. 2 represents again the optical path difference whereas the temporal axis is now vertical. The interference signal is also plotted vertically (left axis). Some regions are marked with RIG to indicate from which of the raw interferograms they originate. For calculating the spectra from the time window interferograms, the center-burst maximum must be included in the interferogram. In the example, this is only the case for the first 101 time windows (Fig. 2).

From Figs. 1 and 2, it becomes obvious that the raw interferograms must be at least partly double-sided. This is necessary to include the center-burst region even for time windows late after the trigger. A doubled-sided section is further needed to perform the phase correction of the transformed spectra [27,28]. But the interferograms do not have to be completely double-sided. However, the timing advance of the trigger in relation to the passage of the center-burst defines the observable experimental time interval. In the described example, the time window interferogram 100 from Fig. 2 is the latest that can be be generated. The reason for this is that the trigger in the first raw interferogram 0 from Fig. 1 has been initiated 100 time windows before the scanning mirror passes the center-burst. Consequently, for allowing the observation of time windows even later than time window 100, more triggers earlier than the first trigger in raw interferogram 0 have to be generated.

2.1. Relations between the TW-FTS parameters

In the following, the most important TW-FTS parameters and their relations are considered. Of particular interest are the total measuring time and the amount of raw data. It is assumed that the relaxation time of the experiment is longer than the scan duration. Therefore, the dynamic experiment can be triggered only once during a scan, which is the case in photolysis experiments. The total number of data points N_S in a double-sided interferogram is given by

$$N_S = \frac{2L}{\Delta x_S} = 4\,L\,\tilde{\nu}_{max} = \frac{2\,\tilde{\nu}_{max}}{\Delta\tilde{\nu}} \quad (1)$$

where L is the maximum optical path difference, Δx_S the optical distance between two sampling points, $\Delta\tilde{\nu} = 1/2L$ the spectral spacing between two adjacent data points in the spectrum, and $\tilde{\nu}_{max}$ the total spectral bandwidth. In addition to the spectral spacing, the temporal resolution is an important characteristic. The temporal distance Δt_S of two neighboring samples in the digitized interferogram is related to the sampling rate $f_S = 1/\Delta t_S$. As stated before, the time windows contain several samples. The duration of one time window Δt_W corresponds to the desired temporal resolution, and $N_{SW} = \Delta t_W/\Delta t_S$ interferogram points are combined to form one time window. For the flash photolysis experiments that are described below, N_{SW} was 8 or 64, respectively (see Table 1). The interferograms are divided into N_{WI} sections of N_{SW} data points each.

$$N_{WI} = \frac{N_S}{N_{SW}} = \frac{2\tilde{\nu}_{max}}{\Delta\tilde{\nu}\,\Delta t_W\,f_S} \quad (2)$$

As illustrated in Figs. 1 and 2, the experiment has to be carried out once for every section. Moreover, since only one experiment per scan can be carried out, N_{WI} equals the number of raw interferograms N_I that have to be recorded. The number of interferograms N_I is an important experimental parameter, because it affects the total measuring time and the amount of data. The total measuring time is given by

$$t_{Meas} = N_I t_{Rel} = \frac{2\tilde{\nu}_{max}}{\Delta\tilde{\nu}\,\Delta t_W\,f_S} t_{Rel} \quad (3)$$

with the experimental relaxation time t_{Rel}. The total amount of data for a complete TW-FTS measurement is calculated by

$$N_{Data} = N_I N_S = \frac{4\tilde{\nu}_{max}^2}{\Delta\tilde{\nu}^2\,\Delta t_W\,f_S} \quad (4)$$

where N_{Data} is the total number of data points. Eqs. (3) and (4) show several ways how to minimize the measuring time and the amount of data. Firstly, the number N_I of experimental repetitions can be reduced by choosing the width of the time windows Δt_W as big as possible. Furthermore, there is a tradeoff between the achievable temporal and spectral resolution. Setting both to the highest values would result in long measuring times and large amounts of interferogram data. The parameters Δt_W and $\Delta\tilde{\nu}$ may probably be chosen arbitrary when preparing the experiment, whereas the sampling rate f_S and the bandwidth $\tilde{\nu}_{max}$ are normally fixed to certain values. In order to keep the amount of data and the measurement time within reasonable ranges, Δt_W and $\Delta\tilde{\nu}$ should be taken as large as possible.

Table 1
Parameters of the validation experiments

	Kinetic experiment	Recording of BrO spectrum
Spectral region covered (cm^{-1})	0–47394	0–47394
Effective spectral resolution (cm^{-1})	40	3.8
Maximum optical path difference (cm)	0.01497	0.17991
Number of interferogram points (single sided)	1419	17053
Number of interferogram points (total)	2838	22746
Sampling frequency (kHz)	24.0	24.0
Temporal resolution (ms)	0.333	2.66
Width of time window (points)	8	64
Number of scans	356	357
Number of observable time windows	178	178
Experimental observation period (ms)	59	474
Relaxation time between two triggers (s)	7.5	7.5
Scan duration (ms)	118	948
Total measuring time (min)	45	45
Total amount of binary data (KB)	3947	31720
Absorption pathlength (cm)	242	962
Br_2 initial concentration (molecules/cm^3)	1.39×10^{16}	2.93×10^{15}
Br initial concentration after photolysis (atoms/cm^3)	2.51×10^{14}	5.27×10^{13}
O_3 initial concentration (molecules/cm^3)	1.20×10^{15}	8.45×10^{15}

2.2. Intensity variations within a time window

In real time-resolved experiments, the conditions are not stable within one time window. The dynamic behaviour leads to slight variations of the light intensity. In a first order approximation, theses changes may be assumed to be linear. Otherwise, the time windows would have been chosen

too wide. Since every section in a time window interferogram is affected by the same intensity change, this results in a sawtooth-like modulation of the time window interferogram. Usually, an intensity modulation of an interferogram is a result of power line effects and unstable analysis light sources, and leads to the so-called ghost spectra [29]. Therefore, the impact of the sawtooth modulation in the TW-FTS interferograms on the spectra was considered analytically and by simulations. It turned out that the intensity variations lead to the appearance of side bands in the transformed time window spectra. The strongest side band is located at a wavenumber distance of $2\tilde{\nu}_{max}/N_{SW}$ to the main spectrum. Fortunately, the side bands appear mainly in the imaginary part of the spectrum, and, with reasonably short time windows, are very weak compared with the main spectrum. As a representative case, an intensity change of 3% within one experimental time window was investigated. The imaginary side bands in an emission spectrum had a strength of 1% in relation to the main spectrum. Yet, the physically relevant real part of the side band was only 0.1%. For absorption spectra, the situation is similar, since only the real parts of the spectra are used for calculating optical densities. The disturbances in the absorption spectra were also about 0.1%.

3. Implementation of the TW-FTS technique

The technique of recording time-windowing interferograms was set up using a commercial Bruker IFS 120 HR Michelson interferometer. Neither software nor hardware changes were made to the FTS. The instrument was operated in a regular measurement mode using the standard software. The built-in analog and digital electronics were used for data recording. As additional hardware, only a timing unit for synchronizing the experiment to the interferometer was needed. The approach is quite general, since it requires only little specific information about the instrument. We expect that the method is easily adaptable to any conventional continuous-scan hardware.

The FTS and the electronic setup that generates the trigger signal are drawn schematically in Fig. 3. The Fourier transform spectrometer is used in a standard continuous-scan

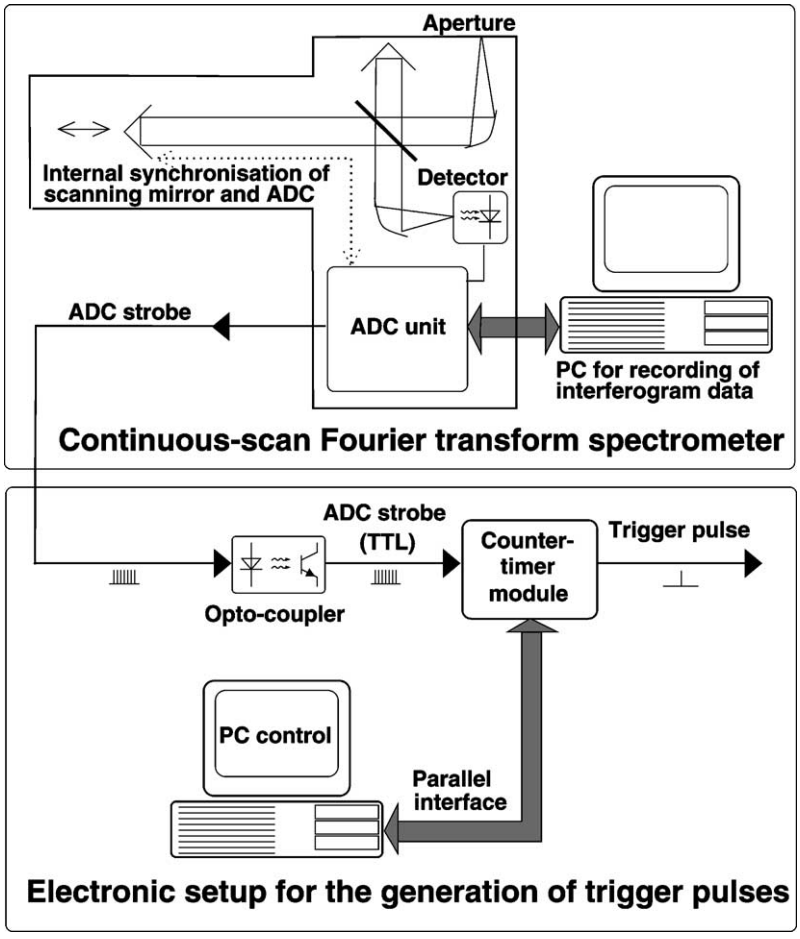

Fig. 3. Scheme of a continuous-scan FTS and the electronic hardware that generates the trigger pulse. The only signal that is needed from the FTS during the measurement is the ADC gate signal. The trigger pulse which is generated by the counter module is used to initiate the observed experiment. For example, the trigger pulse is employed to start the flash driver in the photolysis setup (see Fig. 4).

mode. It is programmed to record a single interferogram, then wait for a certain period which depends on the relaxation time of the observed experiment. The whole procedure is repeated until a complete set of interferogram data files is recorded. The FTS parameters for optics, detector, and filters are set as if performing normal static continuous-scan measurements. Usually, the sampling frequency may also be selected by the spectrometer software. The interferograms are recorded only in one moving direction of the scanning mirror. However, with appropriate software and hardware changes, triggering during both forward and backward movement of the scanning mirror is feasible.

The synchronization signal is generated by counting the gate signals for the analog-to-digital converter that samples the interferogram. The trigger generating electronics work passively, because the timing of the mirror movement is controlled by the FTS. The ADC gate signal is the only hardware signal that is needed from the FTS during the measurement. The counter is programmed via a parallel PC-interface before a scan is started. When the mirror has reached a certain pre-programmed position, a trigger signal is generated. Due to the low experimental repetition rate of about 0.1 Hz only one trigger per FTS scan is produced. Before the next scan, the start value of the counter is changed so that the trigger will be generated at a different optical path difference. Moreover, the counter module is used for a time calibration.

Processing of the recorded set of interferograms is accomplished using a Fortran 90 software on a PC-Linux system. First, the time window interferograms are generated from the recorded raw data. This corresponds to the proceeding from Fig. 1 to Fig. 2. When a series of several time window spectra is generated, all corresponding time window interferograms have to have the same maximum optical path difference. Therefore, all interferograms are shortened to the same length. The resulting time window interferograms typically have the format of time window 100 in the example of Fig. 2. They are single sided, with a short double-sided part. After that the interferograms are apodized and transformed [27]. Since the interferograms are not sampled symmetrically with respect to zero optical path difference, a phase correction of the time window spectra according to the method by Mertz [27,28] is carried out. For TW-FTS spectra, there are two possible ways to determine the phase spectrum. In the first approach, a separate phase spectrum for every time window is calculated from the corresponding time window interferogram. The other approach uses only one phase spectrum for the correction of all time window spectra. It is calculated from one quasi-static scan during the TW-FTS measurement. Both methods of determining the phase spectrum turned out to be equivalent.

For dynamic absorption measurements, a time series of optical density spectra is calculated. As a background spectrum for the optical densities, a negative time window from before the trigger can be used. These time windows have been recorded only a few milliseconds before the actual experiment. Using these negative time windows bears the advantage that artefacts by experimental drifts such as baseline deviations are usually suppressed. This is an important benefit of the TW-FTS compared to conventional FTS techniques.

4. Validation by means of flash photolysis experiments

The presented technique of time-windowing Fourier transform spectroscopy has been used in conjunction with an already existing flash photolysis setup in our laboratory [30,31]. The reactive atmospheric radical BrO has been investigated by the bromine-photosensitized decomposition of O_3. The trigger signal from the TW-FTS was employed to start the photolysis flash, and the formation and decay of BrO after photolysis of a mixture of Br_2 and O_3 was observed by time-resolved absorption spectroscopy. The results of first test measurements at room temperature are reported here. A more thorough study of the UV absorption cross-section of BrO for stratospheric temperatures is being published elsewhere [26].

The flash photolysis setup is sketched in Fig. 4. Since this setup has already been described in [30,31], only a short overview is given here. The Br_2 photosensitized decomposition of ozone was initiated in a temperature-regulated quartz chamber of 3 l volume and 120 cm length. It was used under flow conditions, with gas inflow at on end and pump outlet at the other. The applied gas mixtures contained Br_2, O_3, N_2, and O_2. The reaction vessel was held at a constant temperature of 298 K. Reactions were started by triggering a broadband xenon flash synchronous to the FTS. The flash lamp photolyzed $0.80 \pm 0.11\%$ of the Br_2 molecules, and the created Br atoms almost immediately led to formation of the radical BrO. The gaseous reactions were observed in absorption, using analysis light from a xenon arc lamp (Hamamatsu L2194, 75W) that passed a multi-reflection white optic located in the reaction chamber. After leaving the cell, the analysis light beam was directed to the entrance aperture of the FTS. A GaP detector was employed for the interference measurement.

From the experimental raw interferograms, time window interferograms were generated. These were transformed to yield time window spectra. Then a time series of optical densities was calculated. The intermediate result of the data analysis is plotted in Fig. 5. The diagram shows a temporal series of optical density spectra following the photolysis flash. Almost immediately after the flash at time 0 ms, the formation of BrO can be observed in the wavenumber range from 25,000 to 33,000 cm^{-1}. At the high wavenumber end of the diagram, the Br-catalyzed decrease of the UV absorber O_3 can be monitored by the Huggins absorption bands of O_3 (31,000–36,000 cm^{-1}). The Br_2 absorption on the low wavenumber end remains almost constant, since less than 1% was photolyzed.

Two types of flash photolysis experiments with TW-FTS observation were carried out. The main experimental

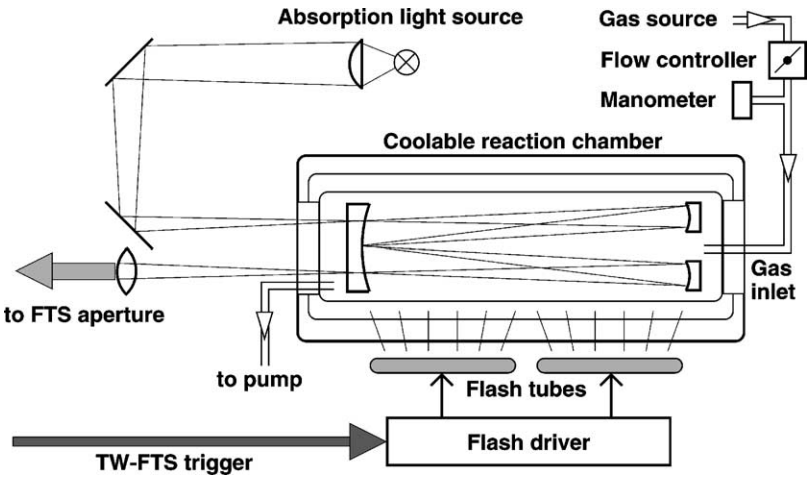

Fig. 4. Flash photolysis setup. The flash driver is triggered by the TW-FTS synchronization signal (see Fig. 3).

parameters are listed in Table 1. The total measuring duration was 45 min for both cases. As pointed out before, the measuring time and the amount of data are limiting factors for the achievable spectral and temporal resolutions.

In the first experiment, the chemical kinetics in the gaseous formation of BrO was observed by time-resolved absorption measurements. The temporal resolution was set to 0.333 ms, and, to limit the measuring time as well as the amount of data, a spectral resolution of 40 cm^{-1} was chosen. For each time window, the concentrations of the absorbers Br_2, BrO, and O_3 were determined. This was done by scaling appropriate reference spectra to the observed optical density. The resulting experimental concentration–time profiles were compared to a chemical kinetics model. The chemical kinetics model consisted of the homogeneous reactions dominating the Br_2/O_3/BrO system as reported by several authors [32–34]. Rate constants were taken from [35] and [33]. The chemical model is also described in detail in [26]. The agreement between experimental and theoretical concentration curves was quite good. The experimental concentration differed from the simulated curve by less than 10% for BrO and by less than 15% for O_3.

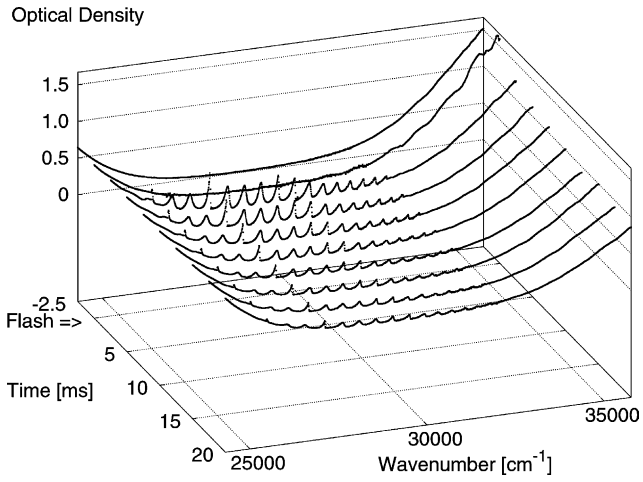

Fig. 5. Time series of optical densities recorded in a flash photolysis of a Br_2/O_3 mixture. The flash has been triggered at time 0 ms. One spectrum every 2.5 ms is shown.

In the second TW-FTS experiment, the UV absorption cross-section of BrO was recorded. It was carried out in order to verify the spectral quality of TW-FTS absorption spectra. A prospective application for the recorded spectra is the data retrieval in atmospheric remote sensing. The spectral resolution was 3.8 cm^{-1}, corresponding to 0.042 nm at 330 nm, which is about a factor of 10 smaller than the typical resolution of atmospheric remote-sensing instruments [36]. In order to limit the amount of data, the time windows were enlarged to 64 interferogram points, corresponding to a temporal resolution of 2.666 ms. In Figs. 6 and 7, the experimental UV absorption spectra of BrO are plotted. Scaling of the optical density spectra to absorption cross-sections was done using results from chemical kinetic experiments [26]. For a comparison, a static FTS spectrum of the same spectral resolution is drawn as well. In the static recording, BrO was produced in a steady flow of O_2, enriched with O_3 and Br_2, through the reaction chamber. Two green fluorescent lamps (Osram L36/66), located near the reaction vessel, photolyzed a part of the Br_2, thus producing Br and further leading to the formation of BrO. However, due to the strong reactivity of BrO, the concentration was rather low, and the maximum optical density was around 0.06. The total measuring time for the static spectrum was 12 h. This duration has to be compared to 45 min recording time needed for obtaining spectra of similar quality using the TW-FTS technique. In time-resolved TW-FTS measurements, on the other hand, optical densities of 0.5 to 1 can be sustained for a period of around 5–10 ms.

Fig. 6 gives an overview of the $A\,^2\Pi_{3/2} \leftarrow X\,^2\Pi_{3/2}$ band system. Due to strong absorption by O_3, the light intensity was very low at wavenumbers higher than 32,000 cm^{-1}, causing an increased noise in this range. The residual in Fig. 6 is slightly shifted to positive values. This points to a

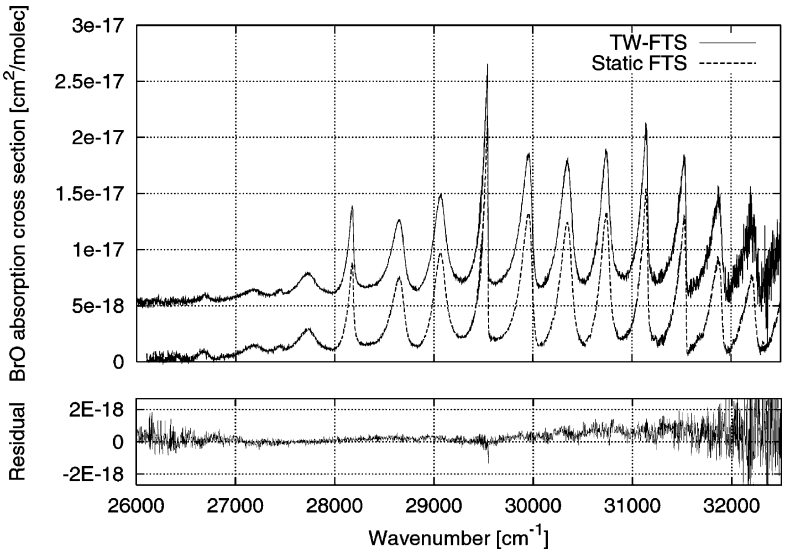

Fig. 6. UV absorption cross-section of the $A\,^2\Pi_{3/2} \leftarrow X\,^2\Pi_{3/2}$ band system of BrO at 298 K. The TW-FTS spectrum (shifted upwards by 5×10^{-18} cm^2 per molecule) is compared to a static FTS recording. The spectral resolution is 3.8 cm^{-1}. The residual has been calculated by subtracting the static spectrum from the TW-FTS spectrum.

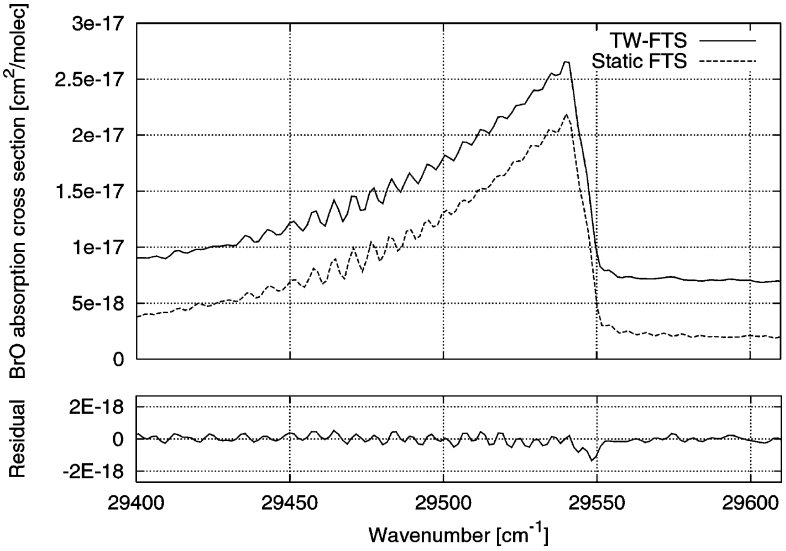

Fig. 7. The (7, 0) vibrational band of the $A\,^2\Pi_{3/2} \leftarrow X\,^2\Pi_{3/2}$ band system of BrO at 298 K. A TW-FTS spectrum (shifted upwards by 5×10^{-18} cm^2 per molecule) is compared to a static FTS recording. The spectral resolution is 3.8 cm^{-1}. The residual has been calculated by subtracting the static spectrum from the TW-FTS spectrum.

baseline deviation in one of the measurements. Due to the larger optical density of BrO in the TW-FTS experiments, a precise determination of a BrO reference spectrum is much easier than in static measurements. Uncertainties in the reference spectra of the other absorbers involved—in this case Br_2 and O_3—have a weaker impact when being eliminated from the time-window spectra. Especially, baseline deviations play a minor role. Apart from the differences in baseline, the two spectra are in good agreement. This is also supported by Fig. 7, which shows the rotational structure of the (7, 0) vibrational band in the $A\,^2\Pi_{3/2} \leftarrow X\,^2\Pi_{3/2}$ electronic transition of BrO. This rotational–vibrational band is one of the few UV bands of BrO that exhibit rotational structure. All observed rotational lines are strongly pre-dissociated [25,37].

5. Conclusion

A new method of time-resolved Fourier transform spectroscopy for a commercial continuous-scan FTS has been presented. The implementation consists of an external synchronization hardware and additional software. No hardware or software changes to the FTS instrument are necessary.

Two flash photolysis experiments were carried out for a validation. They have shown the applicability of the method. In the first experiment, the gaseous reactions in the formation of BrO were observed by time-resolved absorption spectroscopy and compared to a chemical simulation. The second experiment was performed to record a UV absorption spectrum of BrO. The TW-FTS spectrum had a quality comparable to a static recording, but the measurement time was much shorter.

Generally, the advantages of time-resolved and broadband observation methods also apply to the TW-FTS. They have been discussed for the grating spectrograph by Mauldin et al. [38]. Mauldin et al. stressed that the separation of several components in a mixture of absorbers is easier, when a dynamic absorption measurement is carried out. The benefits for the recording of absorption spectra of reactive molecules have also been discussed in [26]. For highly reactive radicals like BrO, larger optical densities can be achieved than in static measurements. Moreover, drifts of the baseline usually play a minor role in time-resolved methods like the TW-FTS compared with the static FTS.

As another interesting technique of time-resolved and broadband optical observation, Rowley et al. [22] presented a grating spectrograph using a CCD detector in a dynamic mode. This setup was used for the investigation of the self-reaction of BrO. The CCD spectrograph may be regarded as being complemental to the TW-FTS. While the advantages of the TW-FTS lie in the spectral calibration and the observable spectral range, the CCD clearly has benefits concerning the measuring time and the sensitivity. This makes it very suitable for the observation of chemical kinetics experiments.

The main limitations of the described TW-FTS method are the amount of produced data and the total measuring time. Usually, one has to decide between a high spectral or a high temporal resolution, since not both are possible in the same measurement. When the experimental repetition rates are above 1 Hz, several triggers during one scan may be generated, thus reducing the amount of data. However, a different technique might be chosen in this case, for example the interleaved continuous-scan without time windows [13]. Moreover, when the experimental repetition rates are high, also the step-scan can achieve high spectral resolutions within a reasonable measuring time [12]. Further, for temporal resolutions below 20 μs the TW-FTS cannot be used, because continuous-scan instruments usually have a maximum sampling rate of 50–100 kHz. Here, the step-scan or the so-called stroboscopic continuous-scan have to be used [13].

The TW-FTS implementation described here is particularly suitable for experiments with a repetition rate of below 1 Hz, at the same time requiring a temporal resolution in the ms to μs range, where the rapid-scan can not be applied. In this parameter range, the time-windowing FTS technique has the advantage of a reduced measuring time in comparison to the step-scan as well as the interleaved continuous-scan as described in [13,16,17]. Flash photolysis experiments fit very nicely in this parameter range. The main applications for the TW-FTS technique will probably be kinetic and spectroscopic investigations in the UV-Vis on the halogen oxides BrO_x and IO_x. Chemical studies may also be supported by time-resolved observations in the infrared, as well as biological and medical experiments with appropriate time constants.

Acknowledgements

This work was accomplished with support from the University of Bremen and the German Space Agency (DARA, Grant no. 50EP9207). Moreover, we gratefully acknowledge technical help by the Bruker Analytik Company in Karlsruhe, Germany.

References

[1] R.J. Bell, Introductory Fourier Transform Spectroscopy, Academic Press, New York, 1972.
[2] J.C. Chamberlain, The Principles of Interferometric Spectroscopy, Wiley, New York, 1979.
[3] A.P. Thorne, Spectrophysics, Chapman & Hall, London, 1988.
[4] S.I. Yaniger, D.W. Vidrine, Appl. Spectrosc. 40 (1986) 174.
[5] H. Sakai, R.E. Murphy, Appl. Opt. 17 (1978) 1342.
[6] W. Barowy, H. Sakai, Infrared Phys. 24 (1984) 251.
[7] G. Hancock, D.E. Heard, Chem. Phys. Lett. 158 (1989) 167.
[8] P. Biggs, G. Hancock, D.E. Heard, R.P. Wayne, Meas. Sci. Technol. 1 (1990) 630.
[9] G. Durry, G. Guelachvili, Appl. Opt. 34 (1995).
[10] W. Uhmann, A. Becker, C. Taran, F. Siebert, Appl. Spectrosc. 45 (1991) 390.
[11] T. Nakano, T. Yokoyama, H. Toriumi, Appl. Spectrosc. 47 (1993) 1354.
[12] N. Picqué, G. Guelachvili, Appl. Opt. 39 (2000) 3984.
[13] J.J. Sloan, E.J. Kruus, Time-Resolved Fourier Transform Spectroscopy, in: R.J.H. Clark, R.E. Hester (Eds.), Advances in Spectroscopy (Time-Resolved Spectroscopy), Wiley, Chichester, 1989, p. 219 (Chapter 5).
[14] G. Hancock, D.E. Heard, Advances in Photochemistry, Wiley, New York, vol. 18, 1993, pp. 1–65.
[15] G.E. Hall, J.T. Muckermann, J.M. Preses, R.E. Weston, G.W. Flynn, Chem. Phys. Lett. 193 (1992) 77.
[16] H. Weidner, R.E. Peale, Appl. Spectrosc. 51 (1997) 1106.
[17] S.A. Rogers, S.R. Leone, Appl. Spectrosc. 47 (1993) 1430.
[18] J. Lindner, J.K. Lundberg, R.M. Williams, S.R. Leone, Rev. Sci. Instrum. 66 (1995) 2812.
[19] S. Voigt, J. Orphal, K. Bogumil, J.P. Burrows, J. Photochem. Photobiol. A 143 (2001) 1.
[20] A. Wahner, A.R. Ravishankara, S.P. Sander, R.R. Friedl, Chem. Phys. Lett. 152 (1988) 507.
[21] O.V. Rattigan, R.A. Cox, R.L. Jones, J. Chem. Soc., Faraday Trans. 91 (1995) 4189.
[22] D.M. Rowley, M.H. Harwood, R.A. Freshwater, R.L. Jones, J. Phys. Chem. 100 (1996) 3020.
[23] M.H. Harwood, D.M. Rowley, R.A. Cox, R.L. Jones, J. Phys. Chem. 102 (1998) 1790.
[24] J.J. Orlando, J.B. Burkholder, A.M.R.P. Bopegedera, C.J. Howard, J. Mol. Spectrosc. 145 (1991) 278.
[25] D.M. Wilmouth, T.F. Hanisco, N.M. Donahue, J.G. Anderson, J. Phys. Chem. 103 (1999) 8935.

[26] O.C. Fleischmann, M. Hartmann, J. Orphal, J.P. Burrows, J. Photochem. Photobiol. A, submitted for publication.
[27] R. Griffiths, J.A. de Haseth, Fourier Transform Infrared Spectrometry, Wiley, New York, 1986, p. 386.
[28] L. Mertz, Infrared Phys. 7 (1967) 17.
[29] R.C.M. Learner, A.P. Thorne, J.W. Brault, Appl. Opt. 35 (1996) 2947.
[30] S. Himmelmann, J. Orphal, H. Bovensmann, A. Richter, A. Ladstätter-Weißenmayer, J.P. Burrows, Chem. Phys. Lett. 251 (1996) 330.
[31] B. Deters, J.P. Burrows, J. Orphal, J. Geophys. Res. 103 (1998) 3563.
[32] S.P. Sander, R.T. Watson, J. Phys. Chem. 85 (1981) 4000.
[33] B. Laszlo, R.E. Huie, M.J. Kurylo, A.W. Miziolek, J. Geophys. Res. 102 (1997) 1523.
[34] A.A. Turnipseed, J.W. Birks, J.G. Calvert, J. Phys. Chem. 94 (1990) 7477.
[35] W.B. DeMore, S.P. Sander, C.J. Howard, A.R. Ravishankara, D.M. Golden, C.E. Kolb, R.F. Hampson, M.J. Kurylo, M.J. Molina, Chemical Kinetics and Photochemical Data for Use in Stratospheric Modeling, JPL Publication 97-4, Jet Propulsion Laboratory, Pasadena, California, 1997.
[36] A. Richter, F. Wittrock, M. Eisinger, J.P. Burrows, Geophys. Res. Lett. 25 (1998) 2683.
[37] M.D. Wheeler, S.M. Newman, T. Ishiwata, M. Kawasaki, A.J. Orr-Ewing, Chem. Phys. Lett. 285 (1998) 346.
[38] R.L. Mauldin, A. Wahner, A.R. Ravishankara, J. Phys. Chem. 97 (1993) 7585.